Compact Three-Dimensional Polymer Waveguide Mode Multiplexer

Dong, Jiangli; Chiang, Kin Seng; Jin, Wei

Published in:
Journal of Lightwave Technology

Published: 15/11/2015

Document Version:
Post-print, also known as Accepted Author Manuscript, Peer-reviewed or Author Final version

Published version (DOI):
10.1109/JLT.2015.2478961

Publication details:
Dong, J., Chiang, K. S., & Jin, W. (2015). Compact Three-Dimensional Polymer Waveguide Mode Multiplexer. *Journal of Lightwave Technology*, *33*(22), 4580-4588. Article 7268783. https://doi.org/10.1109/JLT.2015.2478961

Dong, J., Chiang, K. S., & Jin, W. (2015). Compact Three-Dimensional Polymer Waveguide Mode Multiplexer. Journal of Lightwave Technology, 33(22), 4580-4588. [7268783]. https://doi.org/10.1109/JLT.2015.2478961.

Compact Three-Dimensional Polymer Waveguide Mode Multiplexer

Jiangli Dong, Kin Seng Chiang, *Member, IEEE, Fellow, OSA*, and Wei Jin

***Abstract*—We propose a compact three-dimensional waveguide mode (de)multiplexer based on the configuration of two collocated asymmetrical directional couplers, formed with two dissimilar single-mode cores placed alongside a central rectangular three-mode core in the horizontal and vertical directions, respectively. The waveguides are designed to allow the LP_{11a} and LP_{11b} modes of the central core to completely couple to the LP_{01} modes of the two side cores, respectively, with the LP_{01} mode staying in the central core, which is tapered down at one end to strip off any remaining LP_{11} modes. We fabricate the device with polymer materials by the conventional microfabrication process. A typical fabricated device, which has a total length of 9.0 mm, shows coupling ratios varying from 91% to 99% for the two LP_{11} modes and crosstalks among the modes in the side cores varying from –23.2 to –14.6 dB in the wavelength range 1530 – 1570 nm (the C-band). The crosstalks in the central core are negligible. The insertion loss of the device with fiber leads is about 10 dB and the mode-dependent loss is about ±1 dB. The performance of the device is weakly sensitive to the polarization state of light and insensitive to temperature variations. This device can be used in broadband mode-division-multiplexing transmission systems based on few-mode fibers.**

***Index Terms*—Integrated optics, optical waveguide component, optical planar waveguide coupler, optical polymer, multiplexing.**

I. Introduction

SINGLE-MODE fibers are rapidly approaching their fundamental capacity limit of ~100 Tbit/s set by the fiber fuse phenomenon [1] and the fiber nonlinearity [2]. Mode-division multiplexing (MDM), which allows each mode in a few-mode fiber to carry its own channel, is considered to be an effective technology to increase the signal-carrying capacity of a fiber. With MDM, the transmission capacity of a fiber is increased in proportion to the number of modes that carry independent channels. The key component in an MDM system is a mode (de)multiplexer for launching (separating) different mode channels into (from) a few-mode fiber. In early proof-of-principle MDM experiments, mode (de)multiplexing is realized with phase plates [3] and spatial light modulators [4]. Better performance can be achieved by using multi-plane light conversion [5] or phase plates followed by a Mach-Zehnder interferometer [6]. Such bulk-optic (de)multiplexers can be assembled with readily available optical components, but their disadvantages are obvious: bulky, lossy, and difficult to align. To ease the alignment problem, fiber (de)multiplexers, such as long-period fiber gratings [7,8], photonic lanterns [9,10], and mode-selective fiber couplers [11]–[14], have been demonstrated. To achieve more compact and controllable devices with integration capacity, waveguide-based mode (de)multiplexers have become more popular. Different waveguide structures, such as multimode interferometers [15,16], asymmetric Y-junctions [17,18], and directional couplers [19]–[25] have been proposed for implementing the function of mode (de)multiplexing, among which, directional couplers have attracted more attention for their design flexibility and scalability. For example, an 8-channel hybrid mode (de)multiplexer using six cascaded asymmetric directional couplers fabricated with silicon-on-insulator nanowire waveguides has been demonstrated [21]. While it is relatively easy to (de)multiplex the two degenerate spatial modes of a fiber (e.g., the LP_{11a} and LP_{11b} modes) with fiber (de)multiplexers, such as two orthogonally cascaded symmetric fused-tapered fiber couplers [14] or a photonic lantern formed with carefully arranged fused fiber tapers [9], it is a challenge to (de)multiplex such degenerate modes with an integrated planar waveguide structure.

An approach to (de)multiplexing the LP_{11a} and LP_{11b} modes with planar waveguides is to place an LP_{11}-mode rotator between two asymmetric couplers [22]. The use of an LP_{11}-mode rotator, however, adds complication to the design and the fabrication of the device. A three-dimensional (3D) mode (de)multiplexer fabricated with silicon-rich silica waveguides can (de)multiplex the LP_{01}, LP_{11a}, and LP_{11b} modes, but the crosstalks obtained are high (about –7 dB) [26]. Using the principle of mode coupling in a dissimilar three-core fiber [11], 3D waveguide mode (de)multiplexers [27]–[29] that can (de)multiplex the LP_{01}, LP_{11a}, and LP_{11b} modes have been fabricated in boro-aluminosilicate glass by direct writing with a femtosecond laser. The coupling ratios of such laser-written couplers are yet to be optimized. A high coupling ratio is desirable, as any remained uncoupled power of the mode, if not filtered out at the output, may cause large crosstalks to other modes, or, if filtered out, represents an additional contribution to the insertion loss.

In this paper, we demonstrate a compact 3D polymer waveguide mode (de)multiplexer for the (de)multiplexing of the LP_{01}, LP_{11a}, and LP_{11b} modes, which, like the laser-written

Manuscript received xx 2015. This work was supported by a grant from the Research Grants Council of the Hong Kong Special Administrative Region, China, under Project CityU 112113.

J. Dong, K. S. Chiang, and W. Jin are with the Department of Electronic Engineering, City University of Hong Kong, 83 Tat Chee Ave., Hong Kong, China (e-mail: jldong2-c@my.cityu.edu.hk; eeksc@cityu.edu.hk; weijin@cityu.edu.hk).

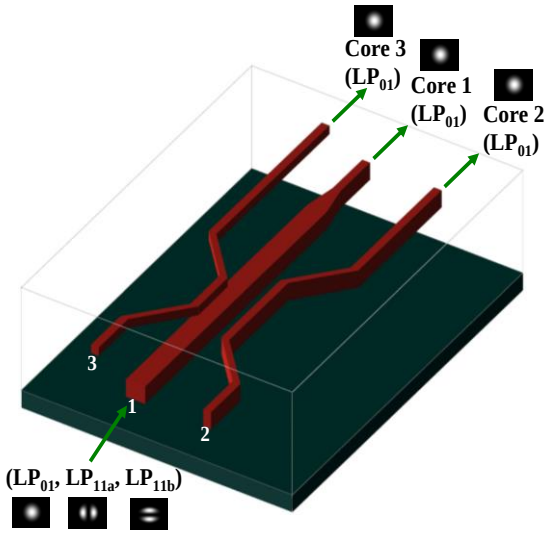

(a)

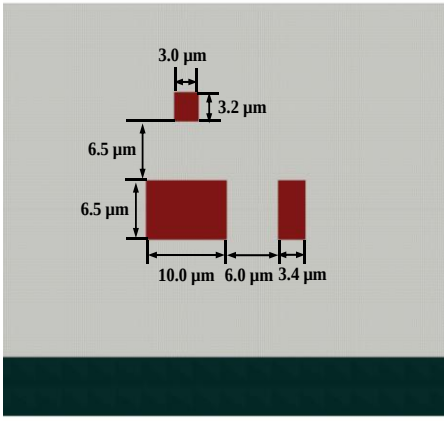

(b)

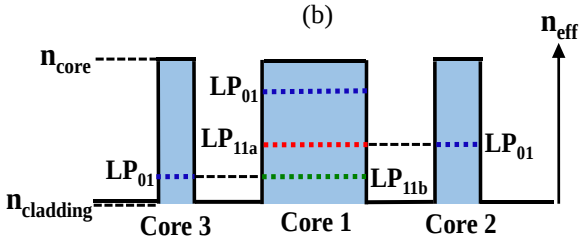

(c)

Fig. 1. (a) The proposed mode (de)multiplexer consists of two collocated horizontal and vertical couplers formed by (b) three dissimilar cores, Core 1, Core 2, and Core3, where (c) the LP_{11a} and LP_{11b} modes of Core 1 are phase-matched with the LP_{01} modes of Core 2 and Core 3, respectively. In (c), n_{core}, $n_{cladding}$, and n_{eff} stand for the refractive indices of the cores and the cladding and the effective index of the mode, respectively.

mode (de)multiplexers [27]–[29], follows the same physics of mode coupling in a dissimilar three-core fiber [11]. Our mode (de)multiplexer consists of two collocated asymmetric directional couplers, which are formed by placing two dissimilar single-mode cores along the horizontal and vertical sides of a central three-mode rectangular core, respectively. The operation principle of the device is based on coupling the LP_{11a} and the LP_{11b} modes from the central three-mode core to the horizontal and vertical single-mode cores, respectively, by taking advantage of the symmetry properties of the modes. To remove any remaining LP_{11} modes in the central core and hence achieve lower crosstalks, the central core is tapered down into a single-mode core at the demultiplexing end. We fabricated the device with polymer materials to take advantage of the microfabrication process based on spin-coating, photolithography, and reactive-ion etching (RIE) for the construction of multilayer 3D structures. The microfabrication process allows precise control of the waveguide dimensions, which is essential for achieving good performance. Our typical experimental device has a total length of 9.0 mm and coupling ratios for the two LP_{11} modes varying from 91% to 99% in the C-band (1530 – 1570 nm). For mode demultiplexing, the crosstalks among the modes in the central core are too small to be measurable (thanks to the taper along the core), while those in the side cores vary from – 23.2 to –14.6 dB in the C-band. The propagation losses of the three modes are lower than 3 dB/cm. The insertion loss of the device with fiber leads is about 10 dB and the mode-dependent loss is about ±1 dB. The characteristics of the device are weakly sensitive to the polarization and insensitive to temperature variations. Its performance is comparable to (if not better than) many other mode multiplexers [19,22,24]. The device can be readily used in broadband MDM transmission systems.

Recently, using the same technology, we demonstrated a mode (de)multiplexer for (de)multiplexing the LP_{01}, LP_{11a}, and LP_{11b} modes without changing the mode patterns [30]. The device, which consists of three identical cores arranged as two cascaded symmetric directional couplers with a total length of 18.5 mm, can find applications where the modes need to be maintained, such as mode routing. On the other hand, the present mode (de)multiplexer incorporates mode conversion, so that the three modes are separated at the demultiplexing ends as the LP_{01} modes. The use of three dissimilar cores to achieve mode-selective phase-matching conditions allows the design with a more compact mode-coupling structure. The device can be used at the transmitter and receiver ends of an MDM system where direct connections to single-mode fiber (SMF) leads are needed. It is possible to integrate more such mode-coupling structures to achieve (de)multiplexing of more modes, which favors the use of more compact structures for increasing the density of integration and lowering the propagation losses.

In comparison with the laser-writing approach [27]–[29], which can be developed into a fast and low-cost process for the realization of 3D waveguide structures but is only applicable to limited photosensitive material systems, our approach based on the well-established microfabrication process can provide a more precise control of the dimensions and the refractive indices of the waveguides and is applicable to a wide range of polymer material. The polymer waveguide technology offers much flexibility in the realization of more sophisticated devices, including thermo-optic and electro-optic devices.

The polymer material used in our work (EpoCore/EpoClad) is highly stable. An imprinting process suitable for mass production of optical printed circuit boards with such polymer has been demonstrated, which involves both high pressure (23 kp/cm^2) and high temperature (up to 245 °C) [31]. The vertical coupler structure used in our design can be formed to a high precision easily with polymer material, but is difficult (or impossible) to form with other popular waveguide material systems (e.g., silicon photonics). In fact, polymer material has

also been employed by others to realize mode-sensitive devices, such as a planar waveguide two-mode switch [32] and a polymer holey fiber coupler [33].

II. Device Structure and Design

Figure 1(a) shows a schematic diagram of our 3D mode (de)multiplexer, which consists of two collocated asymmetric directional couplers arranged in the horizontal and vertical directions, respectively. The two couplers are formed with three parallel dissimilar cores with the central rectangular core (Core 1) supporting the LP_{01}, LP_{11a}, and LP_{11b} modes and the side cores (Core 2 and Core 3) supporting only the LP_{01} mode. Core 1 and Core 2 constitute the horizontal coupler and Core 1 and Core 3 constitute the vertical coupler, as shown in Fig. 1(b). As shown in Fig. 1(a), Core 1 is tapered down into a single-mode core at the demultiplexing end and S-bends are applied at both ends of the device to separate the three cores. We use a rectangular Core 1 for two reasons. First, to facilitate waveguide fabrication, Core 1 and Core 2 should have the same height. If Core 1 had a square shape, Core 2 would have an extremely narrow width to be single-moded, which would be difficult to fabricate. Second, by breaking the degeneracy of the LP_{11a} and LP_{11b} modes, the crosstalk between the two single-mode cores, Core 2 and Core 3, can be substantially reduced, which allows the use of the compact mode-coupling configuration without sacrificing the crosstalk performance.

To facilitate discussions, we consider a demultiplexer, where the LP_{01}, LP_{11a}, and LP_{11b} modes are launched into Core 1 from the three-mode end, as shown in Fig. 1(a). Here we assume that the three cores are sufficiently separated, so that the conventional coupled-mode theory for evanescent-field coupling in a weakly guiding structure is applicable. According to the coupled-mode theory, for any two modes to couple strongly between two parallel cores, the two modes must be phase-matched, i.e., their effective indices must be equal. Because of the rectangular shape of Core 1, the LP_{11a} and LP_{11b} modes have different effective indices. In our case, the cores are designed in such a way that the LP_{11a} mode of Core 1 is phase-matched with the LP_{01} mode of Core 2, while the LP_{11b} mode of Core 1 is phase-matched with the LP_{01} mode of Core 3, as illustrated in Fig. 1(c). For the horizontal coupler, as the LP_{01} and LP_{11b} modes of Core 1 are not phase-matched with the LP_{01} mode of Core 2, together with the fact that the LP_{01} mode of Core 1 is more confined in the core and the LP_{11b} mode of Core 1 has an antisymmetric field distribution in the vertical direction, their couplings to Core 2 are weak. Similarly, for the vertical coupler, the couplings of the LP_{01} and LP_{11a} modes of Core 1 to Core 3 are weak. Therefore, by properly choosing the interaction length between Core 1 and Core 2 and that between Core 1 and Core 3, the LP_{11a} and LP_{11b} modes of Core 1 can couple completely to the LP_{01} modes of Core 2 and Core 3, respectively, while the LP_{01} mode of Core 1 stays in Core 1.

In our design work, we neglect the propagation losses of the modes. The refractive indices of the cores and the cladding are 1.5690 and 1.5590, respectively, which represent the polymer materials used in our experiment. To find the phase-matching conditions, we calculate the effective indices of the modes for various core dimensions with the full-vector finite-element method (COMSOL). Infinite designs are possible with our proposed structure. We present here a typical example to demonstrate our design methodology and practical considerations. For the horizontal coupler, we fix the height of Core 1 and Core 2 at 6.5 μm. Figure 2(a) shows the variation of the effective indices of the LP_{01} and LP_{11a} modes with the core width for a fixed core thickness of 6.5 μm at the wavelength 1550 nm for the TE polarization. The difference in the effective index between the TE and TM polarizations is negligible. As shown in Fig. 2(a), the phase-matching condition for the horizontal coupler is satisfied, when the widths of Core 1 and Core 2 are 10.0 and 3.4 μm, respectively, where the effective indices of the two modes are equal to 1.5625. With the size of Core 1 fixed, we can determine the phase-matching condition for the vertical coupler. There are many possibilities for the dimensions of Core 3. Here the width and the height of Core 3 are chosen to be 3.0 and 3.2 μm, respectively, so that its shape is close to a square. The corresponding effective indices of the LP_{01} mode of Core 3 and the LP_{11b} mode of Core 1 are equal to 1.5602.

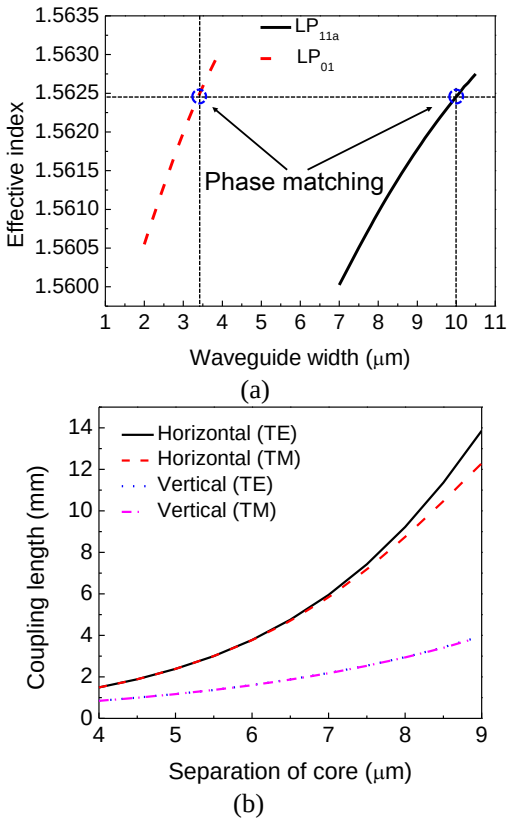

Fig. 2. (a) Variation of the effective index with the core width at a fixed core thickness of 6.5 μm for the LP_{01} and LP_{11a} modes for the TE polarization, showing the core widths required for the two modes to satisfy the phase-matching condition. (b) Variation of the coupling length with the core separation for the horizontal and vertical couplers for the TE and TM polarizations. The results are calculated for the wavelength 1550 nm.

Figure 2(b) shows the coupling lengths of the horizontal and vertical couplers as a function of the core separation for the TE and TM polarizations at the wavelength 1550 nm. The coupling length is the length of the coupler required for the mode of

concern to couple completely from the central core to the respective side core. To determine the coupling lengths of the couplers, we employ the 3D finite-difference beam propagation method (3DFD-BPM) (BeamPROP, RSoft), where the fields of the LP_{11a} and LP_{11b} modes in Core 1 are used, respectively, as the initial conditions. As shown in Fig. 2(b), the coupling length increases with the core separation. For the vertical coupler, the difference in the coupling length between the TE and TM polarizations is hardly visible, while for the horizontal coupler, the polarization dependence becomes significant only at a sufficiently large core separation. We consider serval factors in choosing the core separation. For the vertical coupler, to make it easier to align Core 3 with Core 1 with a microscope in the fabrication process, we prefer a smaller core separation and hence a shorter coupling length. On the other hand, we should use a larger core separation to reduce as much as possible the crosstalks arising from unwanted mode couplings. However, the core separation for the horizontal coupler should not be too large to avoid significant polarization dependence. We finally choose a core separation of 6.0 μm or a coupling length of 3.78 mm for the horizontal coupler and a core separation of 6.5 μm or a coupling length of 1.87 mm for the vertical coupler. In practice, it is impossible to achieve 100% coupling efficiency. To strip off any remaining LP_{11} modes in Core 1, Core 1 is tapered down into a single-mode core at the demultiplexing end, as shown in Fig. 1(a). The taper has a linear profile with a final width of 3.6 μm and a length of 3.0 mm. The dimensions of the cores are shown in Fig. 1(b).

To evaluate the performance of the device, we calculate the coupling ratios and the crosstalks of the couplers by the 3DFD-BPM. The coupling ratios of the horizontal (from Core 1 to Core 2) and vertical (from Core 1 to Core 3) couplers are denoted by $D_{12}(m)$ and $D_{13}(m)$, respectively, where m refers to the mode launched into Core 1 with m = "01", "11a", and "11b" for the LP_{01}, LP_{11a}, and LP_{11b} modes, respectively. The coupling ratios can be expressed as

$$D_{12}(m) = \frac{P_2(m)}{P_{TH}(m)}, \quad (1)$$

$$D_{13}(m) = \frac{P_3(m)}{P_{TV}(m)}, \quad (2)$$

where $P_2(m)$ and $P_3(m)$ are the output powers from Core 2 and Core 3, respectively, when mode m is launched into Core 1, and $P_{TH}(m)$ and $P_{TV}(m)$ are the total output powers from the horizontal and vertical couplers, respectively, when mode m is launched into Core 1.

For the horizontal coupler, the crosstalks from the LP_{01} and LP_{11b} modes launched into Core 1 to the LP_{01} mode of Core 2, denoted as $CT_{12}(01)$ and $CT_{12}(11b)$, respectively, are given by

$$CT_{12}(01) = \frac{P_2(01)}{P_2(11a)}, \quad (3)$$

$$CT_{12}(11b) = \frac{P_2(11b)}{P_2(11a)}, \quad (4)$$

Similarly, for the vertical coupler, the crosstalks from the LP_{01} and LP_{11a} modes launched into Core 1 to the LP_{01} mode of Core 3, denoted as $CT_{13}(01)$ and $CT_{13}(11a)$, respectively, are given by

$$CT_{13}(01) = \frac{P_3(01)}{P_3(11b)}, \quad (5)$$

$$CT_{13}(11a) = \frac{P_3(11a)}{P_3(11b)}. \quad (6)$$

Equations (3)-(6) assume that the powers of the LP_{01}, LP_{11a}, and LP_{11b} modes launched in Core 1 are the same. Because of the taper, the crosstalks in Core 1 can be ignored.

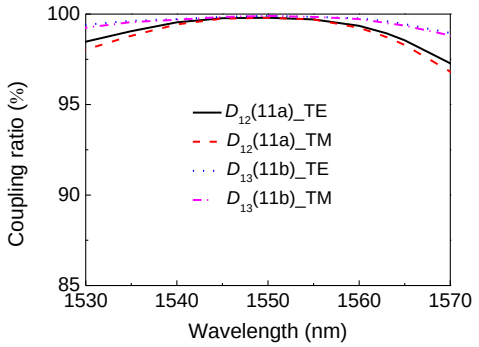

Fig. 3. Calculated coupling ratios from the LP_{11a} and LP_{11b} modes of Core 1 to the LP_{01} modes of Core 2 and Core 3, $D_{12}(11a)$ and $D_{13}(11b)$, for the TE and TM polarizations.

Figure 3 shows the calculated coupling ratios from the LP_{11a} and LP_{11b} modes of Core 1 to the LP_{01} modes of Core 2 and Core 3, i.e., $D_{12}(11a)$ and $D_{13}(11b)$, respectively, for the TE and TM polarizations. The design is optimized at 1550 nm, where the coupling ratios are 100%. Over the C-band (1530 – 1570 nm), the coupling ratio from the LP_{11a} mode of Core 1 to the LP_{01} mode of Core 2 is higher than 93.3% (92.3%) for the TE (TM) polarization, while the coupling ratio from the LP_{11b} mode of Core 1 to the LP_{01} mode of Core 3 is higher than 97.4% (97.1%) for the TE (TM) polarization. The vertical coupler has a higher coupling ratio and weaker wavelength dependence than the horizontal coupler. When the device is operated as a demultiplexer, there exist crosstalks among the mode channels. When the LP_{01}, LP_{11a}, and LP_{11b} modes are launched into Core 1, there are crosstalks from the LP_{01} and LP_{11b} modes of Core 1 to the LP_{01} mode of Core 2 and crosstalks from the LP_{01} and LP_{11a} modes of Core 1 to the LP_{01} mode of Core 3. The crosstalks calculated for the two couplers in the wavelength range 1530 – 1570 nm are shown in Fig. 4(a) and (b), respectively, for the TE and TM polarizations. For the horizontal coupler, as shown in Fig. 4(a), the crosstalks from the LP_{01} and LP_{11b} modes of Core 1 to the LP_{01} mode of Core 2 are smaller than –28.5 (–28.3) and –65.7 (–65.4) dB, respectively, for the TE (TM) polarization. For the vertical coupler, as shown in Fig. 4(b), the crosstalks from the LP_{01} and LP_{11a} modes of Core 1 to the LP_{01} mode of Core 3 are smaller than –20.3 and –34.2 dB, respectively, which are the same for the TE and TM polarizations. The performance of the mode (de)multiplexer is only weakly sensitive to the polarization, thanks to the small index difference between the cores and the cladding. The material dispersion is ignored in our calculation.

According to our calculation, when the dimensions of the cores and the core separations change by ±0.2 μm, the coupling ratios of the couplers are still higher than 92% and the crosstalks are lower than –18 dB in the C-band.

III. FABRICATION

We followed the design parameters given in the previous section to prepare the waveguide masks and fabricated the mode (de)multiplexer by using the micro-fabrication process. We used the polymer materials, EpoCore and EpoClad (Micro Resist Technology GmbH), as the core and cladding materials, respectively, which have excellent processability by photolithography [30,31,34], and applied the spin-coating process to realize the proposed 3D coupling structure.

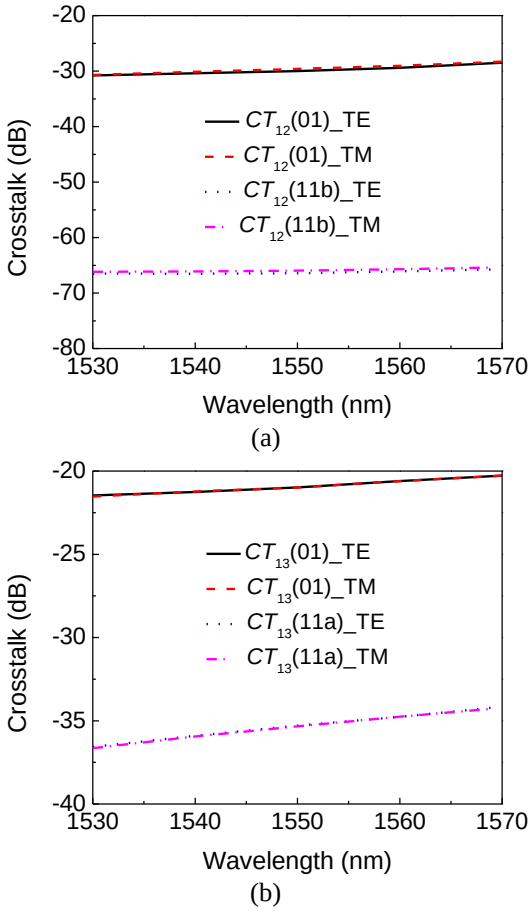

Fig. 4. Calculated crosstalks (a) from the LP_{01} and LP_{11b} modes launched into Core 1 to the LP_{01} mode of Core 2 for the horizontal coupler, $CT_{12}(01)$ and $CT_{12}(11b)$, and (b) from the LP_{01} and LP_{11a} modes launched into Core 1 to the LP_{01} mode of Core 3 for the vertical coupler, $CT_{13}(01)$ and $CT_{13}(11a)$.

The process for the fabrication of the device can be divided into five steps. In the first step, after O_2 plasma cleaning of the surface of the silicon, an EpoClad film was spin-coated and cured on the silicon substrate to form an 18-μm thick under-cladding. In the second step, an EpoCore film was spin-coated and cured on the EpoClad film to form the core layer. The pattern of the horizontal coupler together with the taper was then formed by photolithography. The desired core widths were obtained by carefully controlling the UV radiation for curing and the development and post bake conditions. The desired height of the cores was obtained by oxygen RIE. In the third step, another EpoClad film was spin-coated and cured on the horizontal coupler to form the middle cladding. The fabrication process was the same as that for forming the under-cladding. The required thickness of the middle cladding was obtained by oxygen RIE. In the fourth step, an upper core of EpoCore was formed by using the same process for the formation of the lower cores. In this step, before UV exposure, the positions of the mask and the sample were carefully adjusted with the help of a microscope to achieve precise alignment between the upper and lower cores. In the final step, a 15-μm thick EpoClad film was applied to form the upper cladding. The total length of the device was 9.0 mm. By controlling the curing times in the fabrication process, we were able to control the refractive indices of the polymer materials precisely. The difference in the refractive indices of the polymer materials between the TE and TM polarizations, measured by a prism coupler (Metricon 2010) at 1536 nm, was smaller than 0.001 for both EpoCore and EpoClad, so the material birefringence was small. Microscopic images of the multiplexing and demultiplexing ends of the fabricated device are shown in Fig. 5(a) and (b), respectively. As shown in Figure 5, the three cores are located in two levels. The dimensions of Core 2 and Core 3 remain unchanged at the two ends, while Core 1 has a larger width (10.0 μm) at the multiplexing end to support three modes and a smaller width (3.6 μm) at the demultiplexing end to support only the fundamental mode.

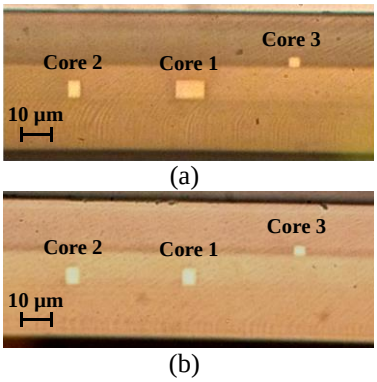

Fig. 5. Microscopic images of the (a) multiplexing and (b) demultiplexing ends of the fabricated device, showing three cores in two levels.

IV. CHARACTERIZATION

To demonstrate the operation of the fabricated device, we launched the LP_{01} modes into the three single-mode cores at the demultiplexing end, respectively, and inspected the modes that appeared at the multiplexing end with an infrared camera. We did the measurements at room temperature. The results obtained at 1550 nm are shown in Fig. 6. The light source used was a pigtailed tunable laser (Agilent 8164B), which could be coupled directly to any core to excite the LP_{01} mode with a high efficiency. When the LP_{01} mode was launched into Core 1, it stayed in Core 1, as shown in Fig. 6(a). When the LP_{01} mode was launched into Core 2, the LP_{11a} mode emerged from Core 1, as shown in Fig. 6(b). When the LP_{01} mode was launched into Core 3, the LP_{11b} mode emerged from Core 1, as shown in Fig. 6(c). The device functioned as a mode multiplexer, as expected.

To better characterize the device, we operated it as a mode

demultiplexer by launching different modes into Core 1 at the multiplexing end and measured the output powers from the three cores at the demultiplexing end. To launch the LP_{11a} or LP_{11b} mode into Core 1, we converted the LP_{01} mode into the desired LP_{11} mode with an all-fiber LP_{01}-LP_{11} mode converter. The mode converter was a CO_2-laser written long-period fiber grating in a two-mode fiber (TMF) (Two-Mode Step-Index Fiber, OFS), which could convert the LP_{01} mode into the LP_{11a} or LP_{11b} mode with a conversion efficiency higher than 99% over the C-band [35]. The output powers from Core 2 and Core 3 at the demultiplexing end can be expressed as

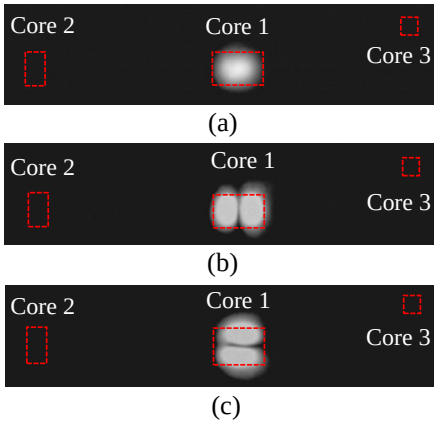

Fig. 6. Near-field images taken at the multiplexing end of the fabricated device at the wavelength 1550 nm, when the LP_{01} mode was launched into (a) Core 1, (b) Core 2, or (c) Core 3 at the demultiplexing end of the device.

$$P_2(01) = P_f(01)C(01)D_{12}(01)\alpha_{12}(01)\,, \quad (7)$$
$$P_2(11\mathrm{b}) = P_f(11\mathrm{b})C(11\mathrm{b})D_{12}(11\mathrm{b})\alpha_{12}(11\mathrm{b})\,, \quad (8)$$
$$P_3(01) = P_f(01)C(01)D_{13}(01)\alpha_{13}(01)\,, \quad (9)$$
$$P_3(11\mathrm{a}) = P_f(11\mathrm{a})C(11\mathrm{a})D_{13}(11\mathrm{a})\alpha_{13}(11\mathrm{a})\,, \quad (10)$$

where $P_f(01)$, $P_f(11\mathrm{a})$, and $P_f(11\mathrm{b})$ are the powers of the LP_{01}, LP_{11a}, and LP_{11b} modes from the input fiber lead, respectively, $C(01)$, $C(11\mathrm{a})$, and $C(11\mathrm{b})$ are the coupling efficiencies of the LP_{01}, LP_{11a}, and LP_{11b} modes from the TMF lead to Core 1, respectively, $\alpha_{12}(01)$ and $\alpha_{12}(11\mathrm{b})$ are the transmission coefficients that account for the losses of the LP_{01} and LP_{11b} modes propagating from Core 1 to Core 2, respectively, and $\alpha_{13}(01)$ and $\alpha_{13}(11\mathrm{a})$ are the transmission coefficients that account for the losses of the LP_{01} and LP_{11a} modes propagating from Core 1 to Core 3, respectively. The above equations are the power-budget formulas for the estimation of the characteristics of the device from the measured output powers. Here we can assume $\alpha_{12}(01) = \alpha_{13}(01)$. We should note that the coupling ratios of the horizontal and vertical couplers, $D_{12}(11\mathrm{a})$ and $D_{13}(11\mathrm{b})$, i.e., the coupling ratios from the LP_{11a} and LP_{11b} modes of Core 1 to the LP_{01} modes of Core 2 and Core 3, respectively, can be readily measured from launching the LP_{01} modes into Core 2 and Core 3 at the demultiplexing end, respectively. By applying the cut-back method to other prepared waveguide samples of the same materials and dimensions, the propagation losses of the LP_{01}, LP_{11a}, and LP_{11b} modes were estimated to be 2.4, 2.7, and 2.9 dB/cm at 1550 nm, respectively, from which we can determine the transmission coefficients of the modes. The slightly larger propagation losses, compared with the figure (~2.0 dB/cm) obtained in our previous device fabricated with the same process and the same material system [30], were mainly due to the longer etching time used in tuning the thicknesses of the cores by RIE, which resulted in more severe surface roughness.

The insertion losses of the device with the TMF and SMF leads connected at the two ends were measured to be about 9.0, 10, and 11 dB for the LP_{01}, LP_{11a}, and LP_{11b} modes, respectively, where the coupling losses of the three modes from the TMF to Core 1 were about 3.5, 4.5, and 6.4 dB, respectively, and the coupling losses from Core 1, Core 2, and Core 3 to the SMFs were about 3.2, 3.3, and 1.7 dB, respectively. The coupling losses could be much reduced by designing (or tapering) the cores to better match the fibers and/or by using fiber tapers and/or an elliptical-core TMF [36] for connection.

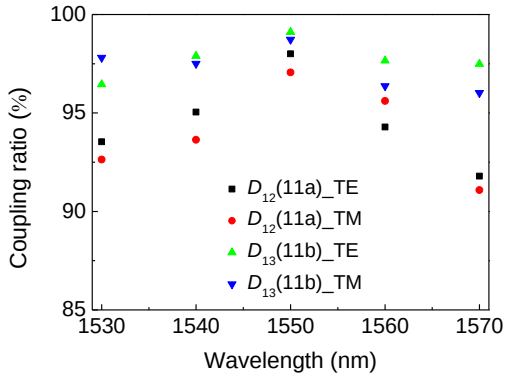

Fig. 7. Coupling ratios from the LP_{11a} and LP_{11b} modes of the central core to the LP_{01} modes of the side cores for the horizontal and vertical couplers, $D_{12}(11\mathrm{a})$ and $D_{13}(11\mathrm{b})$, deduced from the output powers measured for the fabricated device.

The crosstalks from the LP_{01} and LP_{11b} modes launched into Core 1 to the LP_{01} mode of Core 2 are given by

$$CT_{12}(01) = \frac{D_{12}(01)\alpha_{12}(01)}{D_{12}(11\mathrm{a})\alpha_{12}(11\mathrm{a})}\,, \quad (11)$$
$$CT_{12}(11\mathrm{b}) = \frac{D_{12}(11\mathrm{b})\alpha_{12}(11\mathrm{b})}{D_{12}(11\mathrm{a})\alpha_{12}(11\mathrm{a})}\,, \quad (12)$$

and the crosstalks from the LP_{01} and LP_{11a} modes launched into Core 1 to the LP_{01} mode of Core 3 are given by

$$CT_{13}(01) = \frac{D_{13}(01)\alpha_{13}(01)}{D_{13}(11\mathrm{b})\alpha_{13}(11\mathrm{b})}\,, \quad (13)$$
$$CT_{13}(11\mathrm{a}) = \frac{D_{13}(11\mathrm{a})\alpha_{13}(11\mathrm{a})}{D_{13}(11\mathrm{b})\alpha_{13}(11\mathrm{b})}\,. \quad (14)$$

The above equations reduce to Eqs. (3)-(6), when the differences between the propagation losses of the modes are neglected. These equations allow us to deduce the coupling ratios and the crosstalks through selectively launching the LP_{01}, LP_{11a}, and LP_{11b} modes into Core 1 and measuring the corresponding output powers from different cores as well as the output powers from the input fiber lead. Figure 7 shows the coupling ratios for the horizontal and vertical couplers for the TE and TM polarizations, i.e., $D_{12}(11\mathrm{a})$ and $D_{13}(11\mathrm{b})$. As shown in Fig. 7, the coupling ratios are only weakly sensitive to

the polarization. In the wavelength range 1530 – 1570 nm, D_{12}(11a) and D_{13}(11b) are higher than 91.8% (91.1%) and 96.5% (96.0%) for the TE (TM) polarization, respectively. The highest coupling ratios are obtained at 1550 nm, which are 98.0% (97.1%) for the horizontal coupler, and 99.1% (98.7%) for the vertical coupler, for the TE (TM) polarization. The differences in the coupling ratios between the TE and TM polarizations are smaller than 1.4% and 1.5% for the horizontal and vertical couplers, respectively. The vertical coupler has a higher coupling ratio and weaker wavelength dependence than the horizontal coupler, which is consistent with the simulation.

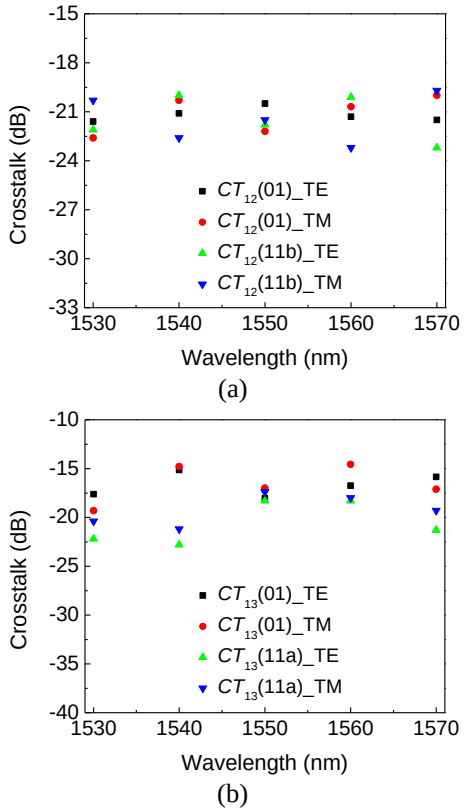

Fig. 8. (a) Crosstalks from the LP_{01} and LP_{11b} modes of Core 1 to the LP_{01} mode of Core 2 for the horizontal coupler, CT_{12}(01) and CT_{12}(11b), and (b) crosstalks from the LP_{01} and LP_{11a} modes of Core 1 to the LP_{01} mode of Core 3 for the vertical coupler, CT_{13}(10) and CT_{13}(11a), deduced from the output powers measured for the fabricated device.

Figure 8(a) and (b) show the crosstalks for the horizontal and vertical couplers in the wavelength range 1530 – 1570 nm, respectively. As shown in Fig. 8(a), the crosstalks from the LP_{01} and LP_{11b} modes of Core 1 to the LP_{01} mode of Core 2 are smaller than –20.5 (–20.0) and –20.0 (–19.7) dB for the TE (TM) polarization, respectively. The lowest crosstalk from the LP_{01} mode of Core 1 to the LP_{01} mode of Core 2 is –21.6 (–22.6) dB at 1530 (1530) nm, while the lowest crosstalk from the LP_{11b} mode of Core 1 to the LP_{01} mode of Core 2 is –23.2 (–23.2) dB at 1570 (1560) nm. As shown in Fig. 8(b), the crosstalks from the LP_{01} and LP_{11a} modes of Core 1 to the LP_{01} mode of Core 3 are smaller than –15.1 (–14.6) and –18.3 (–17.4) dB for the TE (TM) polarization, respectively. The lowest crosstalk from the LP_{01} mode of Core 1 to the LP_{01} mode of Core 3 is –18.0 (–19.3) dB at 1550 (1530) nm, while the lowest crosstalk from the LP_{11a} mode of Core 1 to the LP_{01} mode of Core 3 is –22.8 (–21.2) dB at 1540 (1540) nm. The experimental results agree reasonably well with the simulation.

We also measured the temperature sensitivity of the device by placing a heater under the device to control its temperature. We increased the temperature from 20 to 60 °C and repeated the power measurements as described earlier at different temperatures. Over this temperature range, the coupling characteristics of the device did not change much, except that the location at which the coupling ratios were highest shifted away from 1550 nm at a rate of 2 – 3 nm/°C. As a result, the coupling ratios decreased by 3 – 4% at 1550 nm and the effects on the crosstalk performance are small. The changes in the coupling ratios can be attributed to the small shifts in the phase-matching conditions due to temperature variations. The performance of the device is temperature-insensitive.

On the packaging of the device, fiber pigtails can be formed at both ends of the device with the conventional active alignment process. A precise fiber clamp system developed for polymer waveguides [37] could be incorporated in the device to facilitate connections between the fibers and the cores in different levels.

V. CONCLUSION

We have proposed a compact 3D mode (de)multiplexer based on two collocated asymmetric directional couplers formed with a rectangular three-mode core and two dissimilar single-mode cores. We have presented a specific design for the (de)multiplexing of the LP_{01}, LP_{11a}, LP_{11b} modes and fabricated the device with polymer materials by taking advantage of the spin-coating process for the construction of multilayer 3D waveguide structures. Our fabricated device has a length of 9.0 mm. In the wavelength range 1530 – 1570 nm, the coupling ratios of the couplers vary from 91% to 99% and the crosstalks among the modes in the side cores vary from –23.2 to –14.6 dB (the crosstalks in the central core are negligible). The insertion loss of the device with fiber leads connected at both ends is about 10 dB with a mode-dependent variation of about ±1 dB. The performance of the device is weakly sensitive to the polarization state of light and insensitive to temperature variations. This device can be readily used in broadband MDM transmission systems. The proposed structure offers much flexibility in the design of the waveguides to match the fiber dimensions and minimize the mode-dependent loss. The idea can be extended to (de)multiplexing more modes by cascading more such structures and/or combining our previous structures based on symmetric couplers [30]. However, because of the geometry difference between a rectangular waveguide and a circular fiber, it is a challenge to multiplex a large number of fiber modes with planar waveguide structures [38]. In this regard, we believe that the polymer waveguide technology, which allows the construction of multilayer coupling structures, provides a better solution than other popular waveguide platforms (e.g., silicon photonics). The fiber-waveguide compatibility problem can be alleviated to a certain extent, if elliptical-core few-mode fibers [36], which allow more stable mode propagation, are used for MDM transmission.

REFERENCES

[1] R. Kashyap and K. J. Blow, "Observation of catastrophic self-propelled self-focusing in optical fibers," *Electron. Lett.*, vol. 24, no. 1, pp. 47–49, Jan. 1988.

[2] R.-J. Essiambre , G. Kramer , P. J. Winzer , G. J. Foschini, and B. Goebel "Capacity limits of optical fiber networks," *J. Lightw. Technol.*, vol. 28, no. 4, pp.662–701, Feb. 2010.

[3] V. A. J. M. Sleiffer, Y. Jung, V. Veljanovski, R. G. H. van Uden, M. Kuschnerov, H. Chen, B. Inan, L. G. Nielsen, Y. Sun, D. J. Richardson, S. U. Alam, F. Poletti, J. K. Sahu, A. Dhar, A. M. J. Koonen, B. Corbett, R. Winfield, A. D. Ellis, and H. de Waardt, "73.7 Tb/s (96 x 3 x 256-Gb/s) mode-division-multiplexed DP-16QAM transmission with inline MM-EDFA," *Opt. Express*, vol. 20, no. 26, pp. B428–B438, Dec. 2012.

[4] C. Koebele, M. Salsi, D. Sperti, P. Tran, P. Brindel, H. Mardoyan, S. Bigo, A. Boutin, F. Verluise, P. Sillard, M. Astruc, L. Provost, F. Cerou, and G. Charlet, "Two mode transmission at 2 x 100 Gb/s, over 40 km-long prototype few-mode fiber, using LCOS-based programmable mode multiplexer and demultiplexer," *Opt. Express*, vol. 19, no. 17, pp. 16593–16600, Aug. 2011.

[5] G. Labroille, B. Denolle, P. Jian, P. Genevaux, N. Treps, and J.-F. Morizur, "Efficient and mode selective spatial mode multiplexer based on multi-plane light conversion," *Opt. Express*, vol. 22, no. 13, pp. 15599–15607 Jun. 2014.

[6] K. Igarashi, D. Souma, T. Tsuritani, and I. Morita, "Selective mode multiplexer based on phase plates and Mach–Zehnder interferometer with image inversion function," *Opt. Express*, vol. 23, no.1, pp. 183–194, Jan. 2015.

[7] A. Li, A. Al Amin, X. Chen, and W. Shieh, "Transmission of 107-Gb/s mode and polarization multiplexed CO-OFDM signal over a two-mode fiber," *Opt. Express*, vol. 19, no. 9, pp. 8808–8814, Apr. 2011.

[8] A. Li, X. Chen, A. Al Amin, J. Ye, and W. Shieh, "Space division multiplexed high-speed superchannel transmission over fewmode fiber," *J. Lightw. Technol.*, vol. 30, no. 24, pp. 3953–3964, Dec. 2012.

[9] A. M. Velazquez-Benitez, J. C. Alvarado, G. Lopez-Galmiche, J. E. Antonio-Lopez, J. Hernández-Cordero, J. Sanchez-Mondragon, P. Sillard, C. M. Okonkwo, and R. Amezcua-Correa, "Six mode selective fiber optic spatial multiplexer," *Opt. Lett.*, vol. 40, no. 8, pp. 1663–1666, Apr. 2015.

[10] S. G. Leon-Saval, N. K. Fontaine, J. R. Salazar-Gil, B. Ercan, R. Ryf, and J. Bland-Hawthorn, "Mode-selective photonic lanterns for space-division multiplexing," *Opt. Express*, vol. 22, no. 1, pp. 1036–1044, Jan. 2014.

[11] J. D. Love and N. Riesen, "Mode-selective couplers for few-mode optical fiber networks," *Opt. Lett.*, vol. 37, no. 19, pp. 3990–3992, Oct. 2012.

[12] S. H. Chang, H. S. Chung, N. K. Fontaine, R. Ryf, K. J. Park, K. Kim, J. C. Lee, J. H. Lee, B. Y. Kim, and Y. K. Kim, "Mode division multiplexed optical transmission enabled by all-fiber mode multiplexer," *Opt. Express*, vol. 22, no. 12, pp. 14229–14236, Jun. 2014.

[13] K. Y. Song, I. K. Hwang, S. H. Yun, and B. Y. Kim, "High performance fused-type mode-selective coupler using elliptical core two-mode fiber at 1550 nm," *IEEE Photon. Technol. Lett.*, vol. 14, no. 4, pp. 501–503, Apr. 2002.

[14] A. Li, J. Ye, X. Chen and W. Shieh, "Fabrication of a low-loss fused fiber spatial-mode coupler for few-mode transmission," *IEEE Photon. Technol. Lett.*, vol. 25, no. 20, pp.1985–1988, Oct. 2013.

[15] J. Leuthold, R. Hess, J. Eckner, P. A. Besse, and H. Melchior, "Spatial mode filters realized with multimode interference couplers," *Opt. Lett.*, vol. 21, no. 11, pp. 836–838, Jun. 1996.

[16] T. Uematsu, Y. Ishizaka, Y. Kawaguchi, K. Saitoh, and M. Koshiba, "Design of a compact two-mode multi/demultiplexer consisting of multimode interference waveguides and a wavelength-insensitive phase shifter for mode-division multiplexing transmission," *J. Lightwave Technol.*, vol. 30, no. 15, pp. 2421–2426, Aug. 2012.

[17] J. D. Love and N. Riesen, "Single-, few-, and multimode Y-junctions," *J. Lightwave Technol.*, vol. 30, no. 3, pp. 304–309, Feb. 2012.

[18] W. Chen, P. Wang, and J. Yang, "Mode multi/demultiplexer based on cascaded asymmetric Y-junctions," *Opt. Express*, vol. 21, no. 21, pp. 25113–25119, Oct. 2013.

[19] N. Hanzawa, K. Saitoh, T. Sakamoto, T. Matsui, K. Tsujikawa, M. Koshiba, and F. Yamamoto, "Two-mode PLC-based mode multi/demultiplexer for mode and wavelength division multiplexed transmission," *Opt. Express*, vol. 21, no. 22, pp. 25752–25760, Nov. 2013.

[20] D. X. Dai, J. Wang, and Y. C. Shi, "Silicon mode (de)multiplexer enabling high capacity photonic networks-on-chip with a single-wavelength-carrier light," *Opt. Lett.*, vol. 38, no. 9, pp. 1422–1424, May 2013.

[21] J. Wang, S. He, and D. Dai, "On-chip silicon 8-channel hybrid (de)multiplexer enabling simultaneous mode- and polarization-division-multiplexing," *Laser Photon. Rev.*, vol. 8, no. 2, pp. L18–L22, Mar. 2014.

[22] N. Hanzawa, K. Saitoh, T. Sakamoto, T. Matsui, K. Tsujikawa, M. Koshiba, and F. Yamamoto, "Mode multi/demultiplexing with parallel waveguide for mode division multiplexed transmission," *Opt. Express*, vol. 22, no. 24, pp. 29321–29330, Dec. 2014.

[23] N. Hanzawa, K. Saitoh, T. Sakamoto, T. Matsui, S. Tomita, and M. Koshiba, "Asymmetric parallel waveguide with mode conversion for mode and wavelength division multiplexing transmission," in *Proc. OFC/NFOEC*, 2012, Paper OTu1l.4.

[24] Y. H. Ding, J. Xu, F. D. Ros, B. Huang, H. Y. Ou, and C. Peucheret, "On-chip two-mode division multiplexing using tapered directional coupler-based mode multiplexer and demultiplexer," *Opt. Express*, vol. 21, no. 8, pp. 10376–10382, Apr. 2013.

[25] M. Greenberg and M. Orenstein, "Multimode add-drop multiplexing by adiabatic linearly tapered coupling," *Opt. Express*, vol. 13, no. 23, pp. 9381–9387, Nov. 2005.

[26] T. Hiraki, T. Tsuchizawa, H. Nishi, T. Yamamoto and K. Yamada, "Monolithically integrated mode multiplexer/de-multiplexer on three-dimensional SiOx-waveguide platform," in *Proc. OFC/NFOEC*, 2015, Paper W1A. 2.

[27] S. Gross, N. Riesen, J. D. Love, and M. J. Withford, "Three-dimensional ultra-broadband integrated tapered mode multiplexers," *Laser Photonics Rev.*, vol. 8, no. 5, pp. L81–L85, Sep. 2014.

[28] N. Riesen, S. Gross, J. D. Love, and M. J. Withford, "Femtosecond direct-written integrated mode couplers," *Opt. Express*, vol. 22, no. 1, pp. 29855–29861, Dec. 2014.

[29] S. Gross, N. Riesen, J. D. Love, and M. J. Withford, "C-band mode-selective couplers fabricated by the femtosecond laser direct-write technique" in *Proc. OFC/NFOEC*, 2015, W3B. 2.

[30] J. Dong, K. S. Chiang, and W. Jin, "Mode multiplexer based on integrated horizontal and vertical polymer waveguide couplers," *Opt. Lett.*, vol. 40, no. 13, pp. 3125–3128, Jul. 2015.

[31] W. Jin, K. S. Chiang, K. P. Lor, H. P. Chan, J. T. L. To, and R. H. M. Leung, "Industry compatible embossing process for the fabrication of waveguide-embedded optical printed circuit boards," *J. Lightw. Technol.*, vol. 31, no. 24, pp. 4045–4050, Dec. 2013.

[32] W. Y. Chan and H. P. Chan, "Reconfigurable two-mode mux/demux device," *Opt. Express*, vol. 22, no. 8, pp. 9282–9290, Apr. 2014.

[33] G. Bellanca, N. Riesen, A. Argyros, S. G. Leon-Saval, R. Lwin, A. Parini, J. D. Love, and P. Bassi, "Holey fiber mode-selective fiber couplers," *Opt. Express*, vol. 23, no.15, pp. 18888–18896, Jul. 2015.

[34] R. Himmelhuber, M. Fink, K. Pfeiffer, U. Ostrzinski, A. Klukowska, G. Gruetzner, R. Houbertzb, and H.Wolter, "Innovative materials tailored for advanced microoptic applications," *Proc. SPIE*, vol. 6478, pp. 64780E- 1–64780E-12, Jan. 2007.

[35] J. Dong and K. S. Chiang, "Temperature-insensitive mode converters with CO_2-laser written long-period fiber gratings," *IEEE Photon. Technol. Lett.*, vol. 27, no. 9, pp. 1006–1009, May 2015.

[36] B. Y. Kim, J. N. Blake, S. Y. Huang, and H. J. Shaw, "Use of highly elliptical core fibers for two-mode fiber devices," *Opt. Lett.*, vol. 12, no. 9, pp. 729–731, Sep. 1987.

[37] T. Guan, F. Ceyssens, and R. Puers, "An EpoClad/EpoCore-based platform for MOEMS fabrication," *J. Micromech. Microeng.*, vol. 23, no. 10, pp. 1–10, Oct. 2013.

[38] N. Riesen and J. D. Love, "Few-core spatial-mode multiplexers/ demultiplexers based on evanescent coupling," *IEEE Photon. Technol. Lett.*, vol. 25, no. 14, pp. 1324–1327, Jul. 2013.

Jiangli Dong received the B.S. degree in Physics from Yunnan Normal University, Kunming, China, the M.S. degree in Optics from South China Normal University, Guangzhou, China, in 2009 and 2012, respectively. She is currently working toward the Ph.D. degree at the Department of Electronic Engineering, City University of Hong Kong, Hong Kong.

Her research interests include fiber laser sources, fiber components, and polymer waveguide devices for mode-division-multiplexing applications.

Kin Seng Chiang (M'94) was born in Guangdong, China. He received the B.E. (Hons. I) and Ph.D. degrees in electrical engineering from the University of New South Wales, Sydney, Australia, in 1982 and 1986, respectively.

In 1986, he spent six months with the Department of Mathematics, Australian Defense Force Academy, Canberra, Australia. From 1986 to 1993, he was with the Division of Applied Physics, Commonwealth Scientific and Industrial Research Organization (CSIRO), Sydney, Australia. From 1987 to 1988, he received a Japanese Government research award and spent six months at the Electrotechnical Laboratory, Tsukuba City, Japan. From 1992 to 1993, he worked concurrently for the Optical Fibre Technology Centre, University of Sydney. In August 1993, he joined the Department of Electronic Engineering of City University of HongKong, where he is a Chair Professor. From 2007 to 2010, he was concurrently a Chang Jiang Chair Professor of the University of Electronic Science and Technology of China (UESTC) and is currently associated with UESTC under the Thousand Talents Program. He has published over 450 papers on optical fiber/waveguide theory and modeling, fiber/waveguide characterization, fiber/waveguide devices, optical sensors, optical interconnect, and nonlinear guided-wave optics.

Dr. Chiang is a Fellow of the Optical Society of America and a member of the International Society for Optical Engineering (SPIE) and the Australian Optical Society. He received the Croucher Senior Research Fellowship for 2000–2001. He served as an Associate Editor of *Journal of Lightwave Technology* during 2009-2014 and is currently an editor of *Light: Science & Applications*.

Wei Jin received the B.S. degree in applied physics from Northwestern Polytechnical University, Xi'an, China, the M.S. degree in optics from South China Normal University, Guangzhou, China, and the Ph.D. degree in electronic engineering from the City University of Hong Kong in 2009. Since April 2009, he has been a Research Assistant in the Department of Electronic Engineering, City University of Hong Kong.

His research interests include $LiNbO_3$ and polymer optical waveguide devices.